Measurement of Velocity Field and Turbulent Parameters in a Downward Conical Channel

S. Nuryadin[1*], M. Ignaczak[2], D. Lucas[2], Deendarlianto[1],

[1]Department of Mechanical and Industrial Engineering, Gadjah Mada University, Indonesia

Jln. Grafika No. 2, Kampus UGM – Yogyakarta, 55281

[2]Helmholtz-Zentrum Dresden-Rosendorf, P.O. Box 119, 01314, Dresden, Germany

Abstract: In order to get the deep understanding about the flow structure of the continuous phase in a gas-liquid two phase flow system, an appropriate flow measurement technique has to be performed. In addition, the time and spatial resolution of the technique have to cover the various cases of gas-liquid two phase flow phenomena. However, in case of turbulent flow, the measurement should be able to deliver the detail information about the turbulent parameters as well as its velocity profile. To investigate such case, an experimental investigation to obtain the flow structure in a downward turbulent flow has been carried out in a 288 cm length of conical channel with inlet and outlet diameter of 27.2 mm and 53 mm, respectively. These parameters were measured by using Particle Image Velocimetry (PIV) with microbubbles as the seeding particles. The seeding particles were mixed with the main flow at 50 cm away from the test section and went through the test section homogeneously. The illumination source was a double pulse Nd:YAG laser with wavelength of 532 nm and allow to deliver 200 mJ energy per beam. The high speed camera was also installed synchronously with the laser system in order to record the successive images from both first and second exposure of the laser. Furthermore, the successive images were evaluated by using cross correlation method to extract the velocity data and its fluctuation component. As the result, the velocity field is presented and shows a decrease in axial direction. The normalized turbulent kinetic energy as well as the turbulent intensity in both *x* and *y* direction are also presented. In general, the turbulent intensity increases slightly toward the pipe wall and as it close to the wall, this value increases dramatically. Further, the single bubble with known size was introduced to the test section as an example case to know the effect of the obtained flow field.

Keywords: Particle Image Velocimetry, Turbulent Flow, Turbulent Intensity, Velocity Measurement, Bubble Trajectory.

1. Introduction

The gas-liquid two phase flow phenomena have a substantial interest in variety field of industrial application as well as in basic scientific research. This system can be frequently found in chemical industry, geothermal processes, power plant industry, and many others. For example, the introduced gas in bubble column reactor leads the interaction between gas itself with surrounding liquid where as the result, the mixing process occurred. In such case, the two phase flow knowledge has a great contribution to solve the derived problem and improve the effectiveness as well as the efficiency of the whole process. Moreover, the gas-liquid two phase flow system can deliver the information related to the safety assessment especially in thermal-hydraulic systems which are commonly appear in power plant industries.

However, analyzing the structure of the continuous phase is an important task to give a comprehensive study about the gas-liquid two phase flow structure. Related to this issue, many

*Corresponding author: E-mail: shakti.din@gmail.com; Tel: +62-132-1077851

investigations have been carried out to obtain the information about velocity profile, turbulent parameter, etc with different measurement technique. As the example, a single hot-film anemometer [8] was used to measure the mean and fluctuation of liquid velocity in axial direction while the Reynolds stress components were measured by using a special 3-D conical probe. Another technique can be found in [6] where liquid velocity profile and turbulent parameters were measured with electrodiffusion method. Related to non-intrusive test [1], an experimental investigation to study the turbulence structure in a co-current bubbly flow by using stereoscopic Particle Image Velocimetry (PIV) has been done successfully.

From these measuring methods, the PIV technique is an effective way to obtain the information about the flow field since it is classified to the non-intrusive method. It gives more accurate measurement as long as the seeding particles are able to trace the flow correctly which is related to the Stokes number. Furthermore, it also has an advantage to analyze the transient phenomena from a series of recorded images. In principle, PIV utilizes the characteristic of the neutral particle to trace the flow and the velocity vector is obtained from the displacement of these particles in known measuring frequency. As the result, 2-D velocity field can be derived with single camera or further, a 3-D velocity field with stereoscopic PIV. The use of PIV measurement in two phase flow is varied such as in [4] which was carried out a test of water impingement and used the PIV technique to analyze the observed phenomena. The velocity field as well as the turbulent kinetic energy were extracted successfully. A special technique to measure velocity distribution of gas bubble and liquid phases simultaneously [5] was proposed. The results also showed the capability of their method to extract the information related to the turbulent structure induced by the bubbles. The use of various seeding particle was compared in [3]. The experimental was conducted in a vertical contraction channel by using PIV with microbubble as the seeding particles. They compared the result with the solid particles and showed a similar result although the population of the microbubble was less than the solid particles.

2. Test Facility

The present experiment was carried out at the test facility named “BUTRAJEK”. In general, the test facility is purposed for single bubble experiments. However, the present test is still in frame of these experiments. The test section of the test facility BUTRAJEK was a 288 mm length of conical Plexiglas channel with inlet and outlet diameter of 27.2 mm and 53 mm, respectively. The deionized water as well as the seeding particles flows in downward direction through the conical channel where the measurement takes place. Figure 1 (a) shows the schematic flow of the experiment while figure 1 (b) shows the PIV measurement on test facility. The main flow from the main pump was mixed with the microbubbles at 50 cm above the test section which is allows to produce a homogenously seeding flow. The microbubbles were produced at the microbubbles column and circulated with different pump.

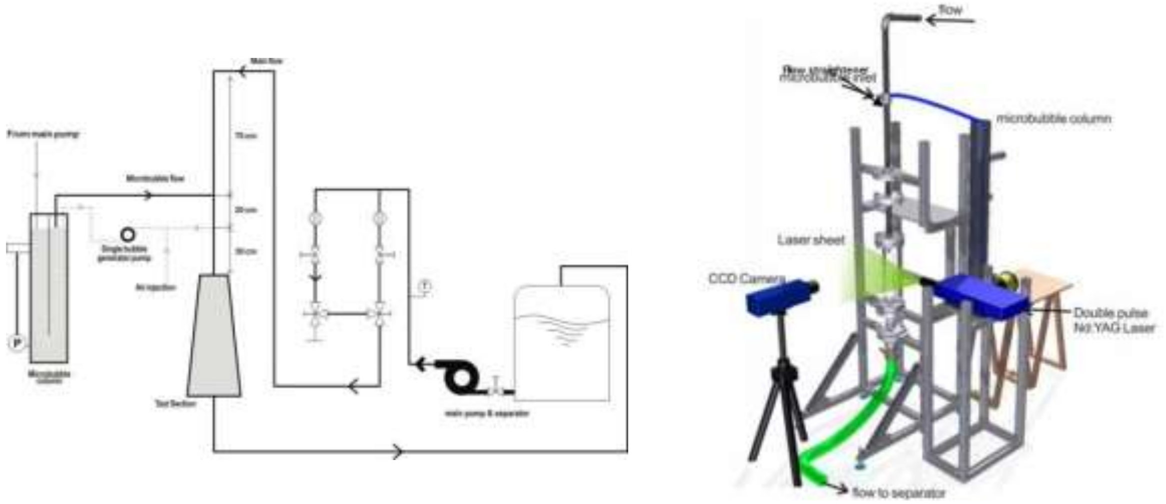

(a) (b)

Figure 1. (a). Flow scheme and (b) PIV measurement on the test section

For the PIV measurement, a double pulsed Nd:YAG laser with 532 nm wavelength was used as illumination source and it delivered 200 mJ energy per beam (with D_{beam} ~5.5 mm). The time delay between two lasers was 2500 µs and the recording device was adjusted to two frames/double exposure mode. This device was a CCD camera with pixel number of 1376(h) x 1040(v) and each pixel has a dimension of 6.45µm x 6.45µm. This camera was synchronized with the laser system and captured the observed phenomena in two successive images, i.e from first and second exposure. The light sheet thickness as well as the divergence angle of the light can be adjusted by refocusing or interchanging the lens. The calibration procedure has been conducted by placing the calibration plate inside the test section which consists of square arrays of 5 mm. A complete calculation of the calibration processes were calculated by the integrated software provided by LaVision.

3. Data Processing

As mentioned in previous chapter, the successive images from the experiment were obtained from a high speed camera which was operated in two frame/double exposure mode. Next, both images from first and second exposure were divided into the "interrogation windows" and the cross correlation method computed all of the interrogation windows where one interrogation window yields one velocity vector. The software package from LaVision was used for this calculation. The first interrogation window size was 64x64 pixels with 50% overlap and a multi pass decreases 32x32 window size with 75% overlap was applied. By using this method, the window shift is improved and the calculated vectors become more reliable. The spatial vector resolution is also improved and the error is less produced. The method is illustrated in figure 2.

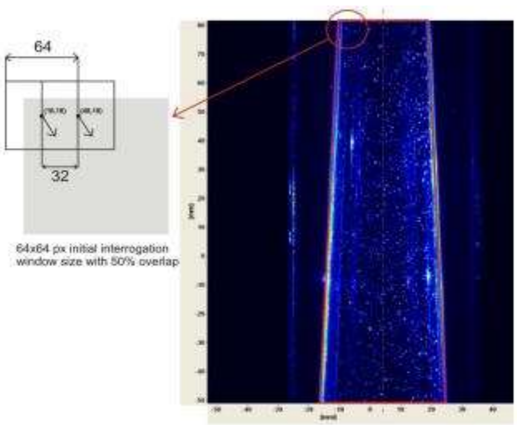

Figure 2. Example of choosen Area of Interest (AOI)

The time averaged velocity field was obtained from the equation (1) while the fluctuation velocity in specified location during measurement time *N* is defined as shown in equation (2).

$$\bar{\ } = \sqrt{\bar{\ }^2 + \ ^2} \quad (1)$$

$$' = \sqrt{\frac{1}{\ } \sum_{t=1} (\ (\ ) - \bar{\ })^2} \quad (2)$$

Equation (2) is the fluctuation velocity component in *x*-direction and it can be extended to *y*-direction with the same procedure. The averaged mean and turbulent kinetic energy are defined as follow,

$$k \ = \frac{1}{2} (\bar{\ }^2 + \ ^2) \quad (3)$$

$$\frac{1}{\ } \ \bar{\ }^2 \ \bar{\ }^2$$

$$k = {}_2(' + ') \quad (4)$$

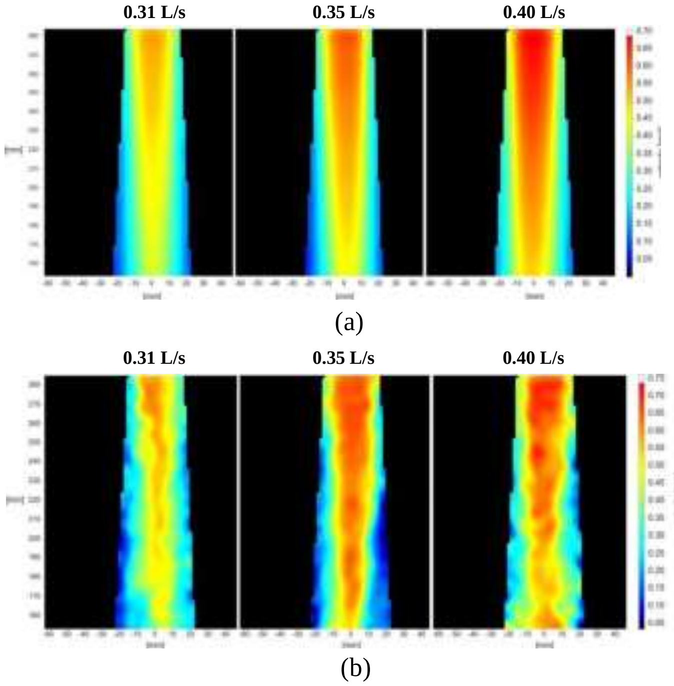

Figure 3. Example of scalar field (a) time averaged velocity and (b) instantaneous velocity for water flow rates of 0.31 L/s, 0.35 L/s, and 0.40 L/s

Based on the method described above, the sample result for time averaged velocity field is shown in figure 3 (a) and a sample of its instantaneous velocity is presented in figure 3 (b). Since the cross section varies in axial direction, the trend of the desired output i.e velocity profile will be presented in five different cross sections. Figure 4 shows these five cross sectional position that will be analyzed further.

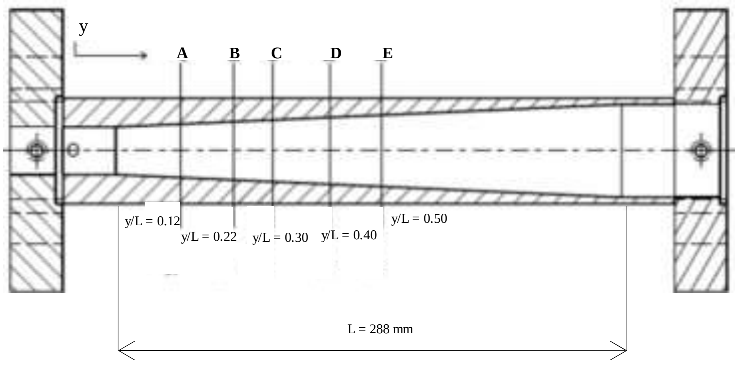

Figure 4. Five different cross sectional cutting

3. Particle Image Velocimetry (PIV) Result

The experiment was carried out in three different flow rates of 0.31 L/s, 0.35 L/s, and 0.40 L/s. Figure 5(a) shows the velocity profile for these flow condition and its development due to varying cross section is also presented based on the segmentation in figure 4. The symmetric velocity profile was achieved for all different flow rates and the velocity decreases as the diameter increases. In general, the decrease of velocity along the selected cross section (A, B, C, D, and E) is about 20% in the pipe center and becomes higher toward the pipe wall, it is observed about 60%. In figure 5(b), the turbulent intensity in *y*-direction has the similar trend for all *y/L* positions in flow conditions. It increases slightly toward the pipe wall and increases dramatically as it closer to the wall. In the pipe center, the turbulent intensity was in range of 5% -8%. The increases of diameter and liquid flow rates have no significant effect in this region.

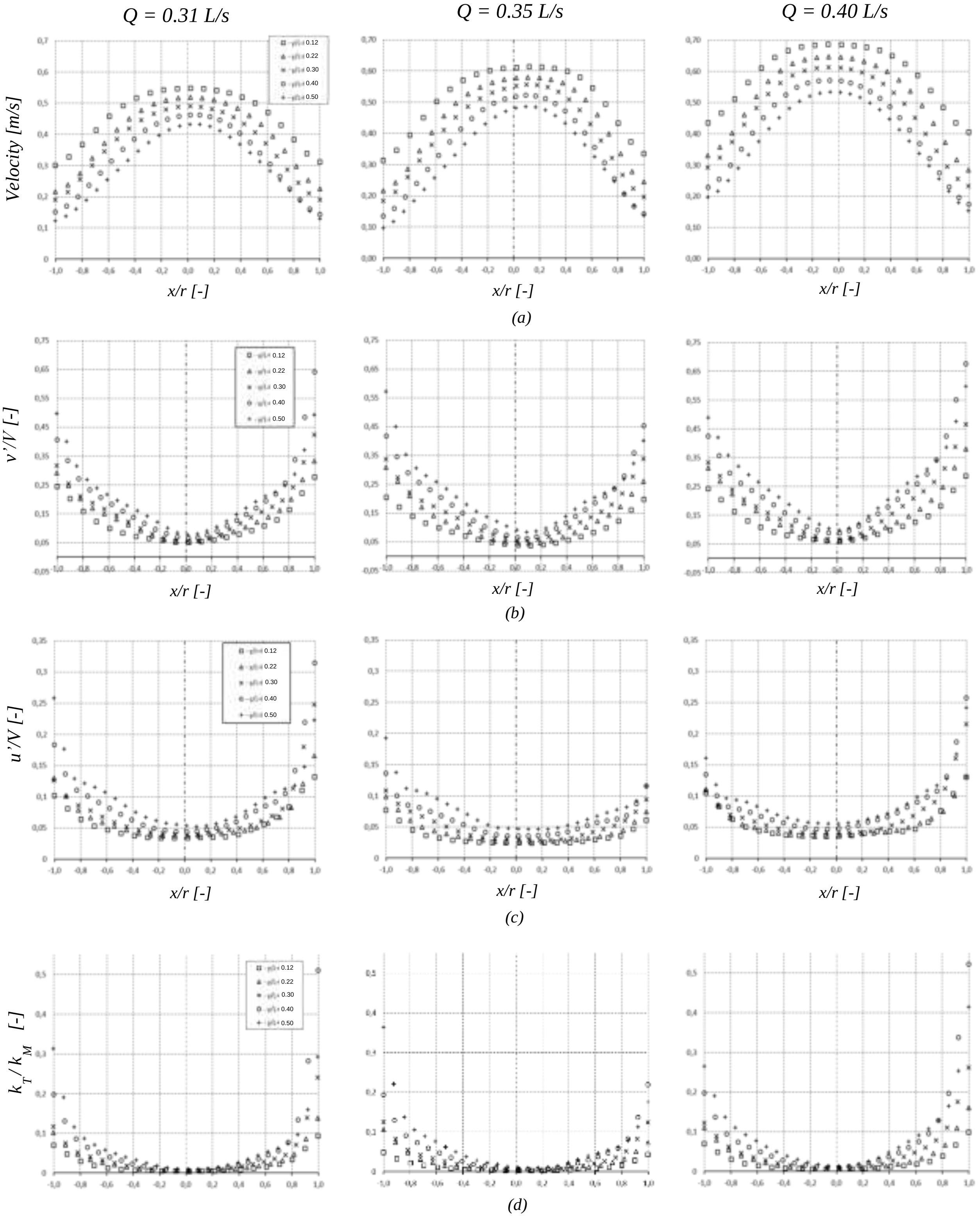

Figure 5. velocity profile (a), turbulent intensity in *y*-direction (b), turbulent intensity in *x* direction (c), and normalized turbulent kinetic energy for three flow rates

The similar result is also found for turbulent intensity in x-direction. As shown in figure 5(c), the turbulent intensity increases slightly toward the pipe wall. At the pipe center, the increasing diameter and liquid superficial velocity have no significant effect. In this region, the turbulent intensity was in range of 3% up to 6%. The highest turbulent level is observed for Q =0.31 L/s and it is started from y/L=0.30 up to y/L=0.50 at x/r=0.9. From this point, the value increases rapidly until the maximum value of about 32 %. Figure 5(d) shows the normalized turbulent kinetic energy to mean kinetic energy. In the pipe center region, the ratio has no more than about 5% while close to the wall (x/r > 0.8) the value of k_T/k_M becomes larger, it is observed in range 30% up to 50%. In general, the present test has a tendency to increase the turbulent level in the wall region. When the water enters the conical channel, it flush out to direction of the wall region and produces high turbulent level on that region due to the divergence angle of the test section.

To check the accuracy of the measurement, a flow rate calculation which depend on velocity profile obtained from figure 5 (a) was performed. The calculation was based on equation 5 and the comparison with the set value of 0.31 L/s, 0.35 L/s, and 0.40 L/s are presented in figure 6. In general, all the data were in overestimate below 10%. The systematic error might be came from some input parameter in PIV calculation i.e *masking*, *image preprocessing*, etc which leads to error in velocity calculation and the fluctuation of flow rate measurement was expected as well.

The flow rate in the test section was calculated according to:

$$Q = \sum_{i=0}^{i=} \pi \ (r)[r_{i+1}^2 - r_i^2] \qquad (5)$$

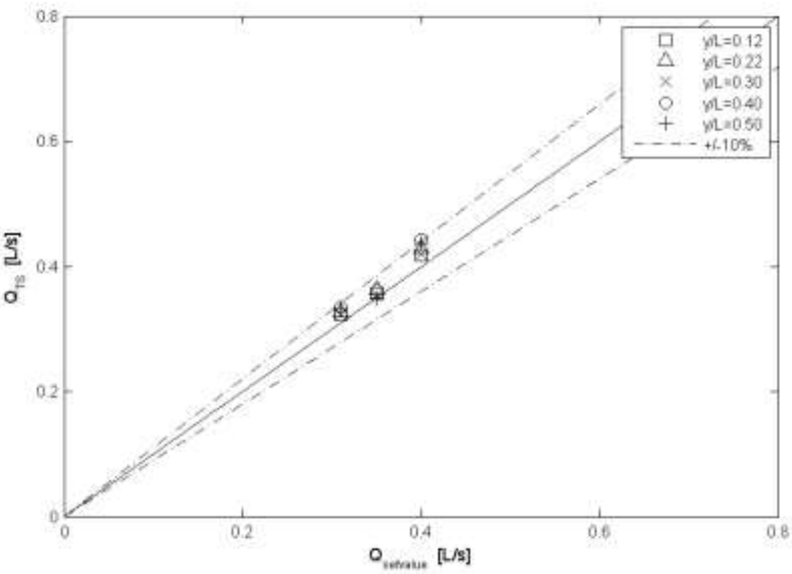

Figure 6. Comparison between set value of liquid flow rate ($Q_{setvalue}$) and liquid flow rate obtained from equation 5 (Q_{TS}) for five different cross sections.

4. Example case: single bubble injection

4.1. Single bubble data processing

To investigate the effect of the flow which has been obtained from the test, the single bubble with known sizes were injected to the test section. The mirror was installed to form 45^o close to the test section to obtain bubble's 3-D position. The measurement of the bubble size took place at the capillary pipe system which was installed before the single bubble entered the test section (dashed line in figure 1.a). The two optical sensors placed at the lower end and upper end of the capillary pipe to measure the bubble velocity and further, to determine its volume inside the capillary pipe. By monitoring the pressure inside the capillary pipe and the test section, the bubble size inside the test section can be determined. By using this method, the bubble sizes for the present case were 6.29 mm and 4.10 mm. The construction and explanation of this system can be found in [2] in detail. The next step is to extract the trajectory of the bubble over the measurement period by using image processing technique. Several investigation related to this technique can be found in literature such as ([10], [11]). For the present test, the bubble's center of mass was detected for each frames and connected to form its trajectory. Figure 6 shows the main steps of this method.

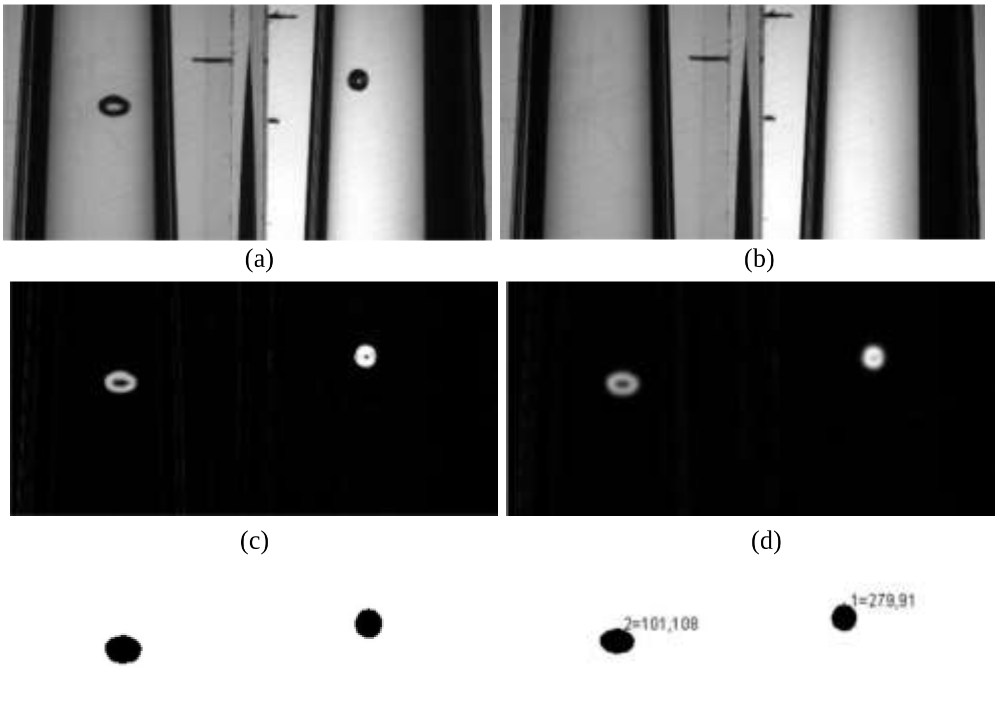

(a) (b)

(c) (d)

(e) (f)

Figure 7. Raw image (a), median image (b), background subtraction result (c), filtering image (d), binarization (e), and center of mass detection (f)

Figure (*7.a)* is the raw image from the experiment while figure (*7.b)* is an image where every pixel on this image contains the median value of all images taken from the experiment. In figure (*7.c)*, the image subtraction is applied between all images (raw images) in figure (*7.a)* to the median image in figure (*7.b)*. Due to presence of the noises, the image filtering was applied by using Gaussian blur method and its result is shown in figure (*7.d)*. Next, a threshold value was given and filling algorithm was performed to fill the region inside the bubble which has higher grayscale value due to light reflection. As the result, a binary can be determined as shown in figure (*7.e)* and the center of mass was assigned to the bubble in each frame as shown in figure (*7.f)*.

4.2. Bubble trajectory

Figure 8 shows the trajectory of the bubble under liquid flow rate of 0.3 L/s with bubble equivalent diameter of 6.29 mm. The bubble fluctuates near the wall region frequently while it went through the lower part of the test section in short frequency. The dis-continue trajectory line appears due to poor illumination source which leads to the bad binarization. However, the bubble was not captured in long time period in that region.

As mentioned in previous chapter, the flow structure has an effect to the movement or fluctuation of the dispersed phase i.e to the single bubble. It should be a starting point to analyze the whole phenomena. In the present case, a higher turbulent level in the wall region was observed. The test section construction which has a divergence angle gives a contribution as well to increase the turbulent level. This condition leads to the obtained bubble trajectory as shown in figure 8. In such flow structure as shown in figure 5, there is a possibility that the bubble will fluctuate in certain radial position.

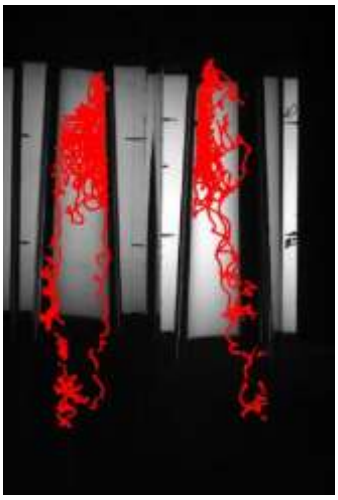

Figure 8. Bubble trajectory (D_b = 6.29 mm, Q = 0.3 L/s)

5. Conclusion

The measurement of velocity fields as well as turbulent parameters in downward conical channel has been presented successfully. The measurement was conducted by using PIV with microbubbles as the seeding particle. In general, the velocity decreases about 20% in the pipe center up to 60% in the region near the wall. The turbulent intensity as well as normalized turbulent kinetic energy have no significant effect in the pipe center region. However, the turbulent intensity and normalized turbulent kinetic energy were observed increase dramatically near the wall up to 32% and 50%, respectively. As a sample case, the single bubble was injected through the test section under flow rate of 0.3 L/s in order to know the effect of obtained flow structure. The result showed that the trajectory of the bubble was observed to fluctuate in long time period in the pipe wall region.

6. References

[1] Hassan, Y. A., W. Schmidl, and J. O. Villafuerte. Investigation of three dimensional two phase flow structure in a bubbly pipe flow, Meas. Sci. Technol. 1997:(9) 309-326.

[2] Ignaczak, M., Experimentelle Untersuchung der Lateralen Liftkraft, Technische Univertitat Dresden. 2012.

[3] Ishikawa, M., K. Irabu, I. Teruya, and M. Nitta. PIV measurement of a contraction flow using micro bubble tracer, J.Phys. 2009; Conf. Ser. Vol 147.

[4] Kendil, F. Z., Danciu, D. V, Schmidtke. M, Bousbia. A. S, Lucas. D, Krepper. E, Mataoui. A. Velocity field under impinging jets with gas entrainment, Progress in Nuclear Energy. 2012: (56) 100-110.

[5] Lindken R., Merzkirch W. A novel PIV technique for measurements in multiphase flows and its application to two-phase bubbly flows, Experiments in Fluids, 2002:(33) 814–825

[6] Nakoryakov. V. E., O. N. Kashinsky, V. V. Randin, L. S. Timkin. Gas-liquid bubbly flow in vertical pipes, Journal of Fluids Engineering. 1996 Vol. 118

[7] Raffel. M, Willert. C. E, Wereley. S. T, Kompenhans. J. Particle Image Velocimetry, A Practical Guide, Springer-Verlag Berlin. 2007.

[8] Wang, S. K., Lee, S.J, Jones Jr, O.C, and Lahey Jr. R.T. 3-D turbulence structure and phase distribution measurements in bubbly two-phase flows, Int. J. Multiphase Flow. 1987:(13) 327-343.

[9] Wilcox, D. C. Turbulence modeling for CFD, DCW Industries, Inc. 1993.

[10] Zaruba, A., E. Krepper, H.-M.Prasser, B.N.Reddy Vanga. Experimental study on bubble motion in a rectangular bubble column using high-speed video observations, Flow Measurement and Instrumentation. 2005:(16) 277–287

[11] Zaruba, A., E. Krepper, H.-M.Prasser, E. Schleicher. Measurement of bubble velocity profiles and turbulent diffusion coefficients of the gaseous phase in rectangular bubble column using image processing, Experimental Thermal and Fluid Science. 2005:(29) 851–860

Acknowledgement

Special thanks for TOPFLOW crew who involved on this work. Tobias Seidel, Thomas Geissler, and Thomas Barth.